DOI: 10.22449/2413-5577-2022-2-38-52

Variability of Marginal Ice Zone Characteristics and Internal Wave Field near Svalbard according to Sentinel-1 Satellite Data

T. V. Mikhaylichenko *, L. A. Petrenko, I. E. Kozlov

Marine Hydrophysical Institute of RAS, Sevastopol, Russia
** e-mail: fsbsi.mhi.tamara@yandex.ru*

Abstract

The paper presents the results of observations of the ice edge drift and surface manifestations of short-period internal waves according to *Sentinel-1 A/B* spaceborne synthetic aperture radar data in June – September 2019. We analyzed 1200 spaceborne synthetic aperture radar images used to record the ice edge position and 387 surface manifestations of short-period internal waves. During the study period in 2019, the maximum southern position of the drifting ice edge in Fram Strait at 79° N was recorded on 20 June. The ice edge boundary reached its maximum northern position at 82° N on 16 September. The seasonal decrease in ice area in the study region was more intensive in the southeastern sector. The largest number of surface manifestations of short-period internal waves was detected in August: 162 packets. The maximum probability of short-period internal waves during the study period was observed in the shelf areas to the northwest and south of Svalbard. Internal waves were observed as packets of 4–5 waves. The maximum lengths of the leading wave front were 30–40 km and were observed to the south of Svalbard. Short-period internal waves with leading wave front lengths of 7–10 km prevailed. The highest probability was noted for waves with a packet width of 3–4 km. The paper presents detailed maps of the internal waves' probability and the spatial distribution of their main parameters. The paper analyzes the relationship between the variability of internal wave parameters and that of the ice edge. It is shown that density gradients resulting from ice melting at the ice edge affect the generation and propagation of short-period internal waves. The combination of the melting process, tidal currents and influence of the bottom topography leads to the generation of large packets of short-period internal waves.

Keywords: short-period internal waves, spaceborne radar images, marginal ice zone, Svalbard, Fram Strait

Acknowledgements: the research of spatial-temporal variability of the internal wave field was performed under state assignment of FSBSI FRC MHI on topic no. FNNN-2021-0010. The analysis of spatial-temporal variability of the marginal ice zone and its relationship with the internal wave field was performed under grant no. 21-17-00278 of the Russian Science Foundation.

For citation: Mikhaylichenko, T.V., Petrenko, L.A. and Kozlov, I.E., 2022. Variability of Marginal Ice Zone Characteristics and Internal Wave Field near Svalbard according to Sentinel-1 Satellite Data. *Ecological Safety of Coastal and Shelf Zones of Sea*, (2), pp. 38–52. doi:10.22449/2413-5577-2022-2-38-52

Изменчивость характеристик прикромочной ледовой зоны и поля внутренних волн у архипелага Шпицберген по спутниковым данным Sentinel-1

Т. В. Михайличенко *, Л. А. Петренко, И. Е. Козлов

Морской гидрофизический институт РАН, Севастополь, Россия
** e-mail: fsbsi.mhi.tamara@yandex.ru*

Аннотация

Представлены результаты наблюдений за кромкой поля дрейфующих льдов и поверхностными проявлениями короткопериодных внутренних волн по данным спутниковых радиолокаторов с синтезированной апертурой *Sentinel*-1 *A/B* в июне – сентябре 2019 г. Проанализировано 1200 изображений спутниковых радиолокаторов с синтезированной апертурой, на которых фиксировалось положение границы распространения льдов и было зарегистрировано 387 поверхностных проявлений короткопериодных внутренних волн. В рассматриваемый период 2019 г. максимально южное положение кромки поля дрейфующих льдов в проливе Фрама на 79° с. ш. зафиксировано 20 июня. Крайнего северного положения на 82° с. ш. граница льдов достигла 16 сентября. Сезонное уменьшение количества льда на рассматриваемой акватории происходило более интенсивно в юго-восточном секторе. Наибольшее количество поверхностных проявлений короткопериодных внутренних волн выявлено в августе – 162 пакета. Максимальные значения повторяемости короткопериодных внутренних волн за рассматриваемый период отмечались в шельфовой области к северо-западу и к югу от архипелага Шпицберген. Внутренние волны наблюдались в виде пакетов из 4–5 волн. Максимальные значения длины фронта лидирующей волны составляли 30–40 км и наблюдались к югу от архипелага Шпицберген. Преобладали короткопериодные внутренние волны с длинами фронта лидирующей волны 7–10 км. Наибольшая повторяемость отмечена у волн с шириной пакета 3–4 км. Представлены детальные карты повторяемости внутренних волн и пространственного распределения их основных параметров. Проанализирована связь изменчивости параметров внутренних волн с изменчивостью границы распространения льдов. Получено, что плотностные градиенты, возникающие при таянии льда на кромке ледового поля, оказывают влияние на генерацию и распространение короткопериодных внутренних волн. Сочетание процесса таяния льда, приливных течений и влияния донной топографии приводит к генерации крупных пакетов короткопериодных внутренних волн.

Ключевые слова: короткопериодные внутренние волны, спутниковые радиолокационные изображения, прикромочная ледовая зона, архипелаг Шпицберген, пролив Фрама

Благодарности: исследование пространственно-временной изменчивости поля внутренних волн выполнено в рамках государственного задания ФГБУН ФИЦ МГИ по теме № FNNN-2021-0010, анализ пространственно-временной изменчивости прикромочной ледовой зоны и ее связи с полем внутренних волн выполнен в рамках гранта РНФ № 21-17-00278.

Для цитирования: *Михайличенко Т. В., Петренко Л. А., Козлов И. Е.* Изменчивость характеристик прикромочной ледовой зоны и поля внутренних волн у архипелага Шпицберген по спутниковым данным *Sentinel*-1 // Экологическая безопасность прибрежной и шельфовой зон моря. 2022. № 2. С. 38–52. doi:10.22449/2413-5577-2022-2-38-52

Introduction

Currently, there is still interest in the study of internal waves (IWs) in the Arctic seas. Along with studies carried out on the basis of in situ measurements [1–4], satellite observations make it possible to obtain a picture of the spatial distribution of sources of internal wave generation in the entire ice-free water area of the Arctic Ocean. At the moment, studies have been carried out to identify IWs and assess their characteristics with regard to a number of the Arctic seas [5–8]. Yet, the water areas, which are adjacent to Svalbard, were not considered in an integrated manner. At the same time, the waters near the archipelago are characterized by special hydrological parameters, complex system of heat transfer with currents, and constant removal of drifting ice from the northern polar region through Fram Strait [9–11]. Thus, combination of complex bottom topography and tidal water movements near Svalbard establish all the conditions for the possible generation of IWs. According to the results of modeling and in situ measurements made to the north and southeast of the archipelago, short-period IWs (SIWs) were found [1, 8, 12, 13]. In the region under consideration, on the basis of successive measurements of spaceborne synthetic aperture radars (SARs), surface manifestations of SIWs were also identified, and their phase velocities were determined [14].

Nevertheless, a comprehensive study of the sources of generation and propagation of the SIWs near the archipelago and adjacent Fram Strait was not carried out. In this regard, the purpose of this paper is to determine key regions of generation and main spatiotemporal characteristics of the SIWs near Svalbard and in Fram Strait based on the analysis of the array of *Sentinel-1 A/B* satellite SAR images and the consideration of the relationship between the SIW characteristics and the boundary of the drifting ice field in the warm period of 2019.

Data and methods

To analyze the spatial variability of the SIW field in Fram Strait and Svalbard shelf area, *Sentinel*-1 *A/B* radar images (RI) for June – September 2019 from the archives of the *Copernicus Open Access Hub* system of the European marine forecast centers (https://scihub.copernicus.eu) were used.

According to SAR images, the ice edge position and surface manifestations of the SIWs (SM of SIWs) were recorded. Analysis and identification of internal waves in SAR images were carried out in accordance with the technique described in [6]. 1,200 SAR images were analyzed in total, on which 387 SM of SIW were identified. The ice edge position reflecting the ice – open water boundary without taking into account ice concentration was taken as the ice edge.

SAR images were analyzed using *SNAP © ESA* (*Sentinel Application Platform*) program (https://step.esa.int/main/toolboxes/snap/). This software makes it possible to perform preliminary processing and visualization of SAR images, select the part of interest of the image, draw a section through the SIW packet and determine its main spatial characteristics – the leading wave front length and the packet width.

The procedure of the SAR images analysis was carried out in two stages. At the first stage, the SAR images were subjected to low-pass filtering, i.e., spatial variations of the radar signal field on scales much larger than the IW length were excluded. After this procedure, the manifestations of IW packets on SAR images became more contrasting, and then they were subjected to quantitative analysis.

Fig. 1 shows an example of the IW manifestation on SAR image in the form of three successive packets of SIW. Curve *A–B* is the front length of the leading wave, which made 17.8 km; segment *C–D* is the SIW packet length, which made 11 km. As for the second packet, the front length of the leading wave made 47.4 km, and the SIW packet length made 15 km. The front length of the third packet leading wave made 61.4 km, and the SIW packet length made 15 km.

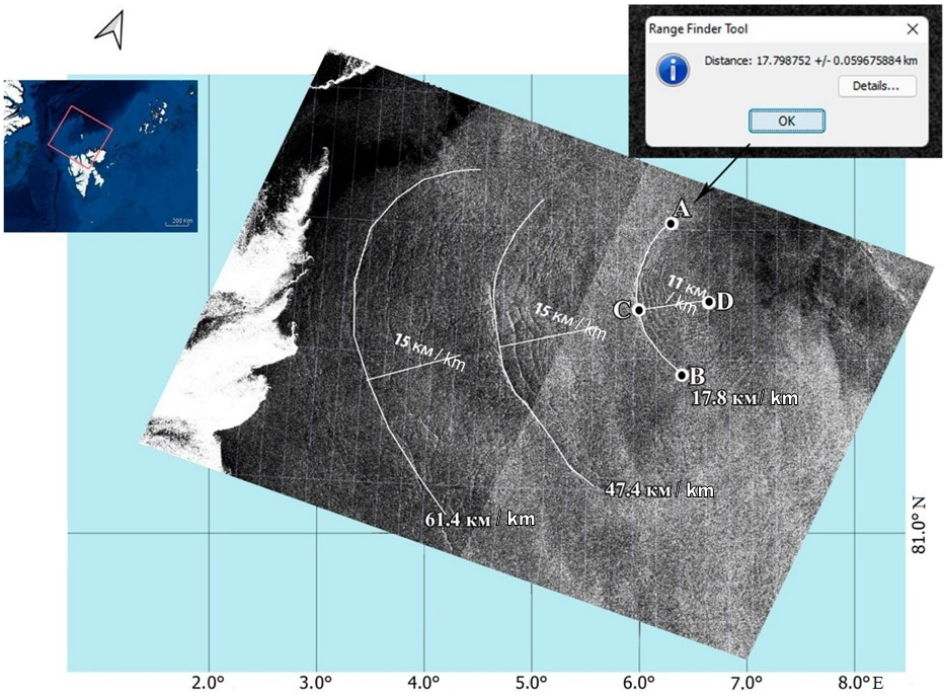

F i g . 1 . Enlarged fragment of the original *Sentinel-1 B* SAR image of 15 August 2019 with manifestation of three successive packets of SIWs. *A–B* is the front length of the leading wave of the SIW packet; *C–D* is the SIW packet length

Processing of the analysis results and construction of the spatial maps of various SIW characteristics were carried out in the *MathWorks © Matlab* environment.

Variability of the ice edge position

Since the identification of the SM of SIWs is possible only in open water, the ice edge drift position was recorded using the SAR images in order to obtain a general picture of the ice conditions in the study area.

During the study warm period in 2019, the difficult ice conditions in the region took place due to the abnormally increased frequency of atmospheric processes of the eastern (*E*) and meridional (*C*) circulation forms and the intensive transfer of ice from the northern polar area. At the same time, southeasterly and southerly winds prevailed at a speed of up to 6–7 m/s. At the end of the period, in the second half of September, northerly and northwesterly winds with a speed of 7–8 m/s dominated [1].

At the beginning of June 2019, the ice edge adjoined the northern coast of Svalbard. The ice spread along the eastern coast of the archipelago up to 75° N (Fig. 2, *a*). To the south of Svalbard, the ice occupied the entire space from 17° E and further eastwards.

In the following days, unlike in previous years, the ice continued to move southward to Fram Strait and by 20 June 2019, near the western coast of the archipelago, it reached its maximum southern position at a latitude of 79° N. At the same time, extended polynyas lying beyond the island were formed on the eastern side of the archipelago, in the ice field. At the end of June, the direction of the general ice drift changed and the ice edge started to move slowly backward to the north.

In early July 2019, ice near the northern coast of Svalbard diverged. By the end of July 2019, the area of open water expanded eastward to Hinlopen Strait (22° E). To the north, the ice edge drift moved slightly, not reaching 81° N. In the south, the ice field shifted to the southern extremity of Edge Island, i.e. to 77° N (Fig. 2, *b*).

The seasonal decrease in the amount of ice in the region under consideration was more intense in the southeastern sector. By the end of August (see Fig. 3, *a*), the ice remained only off the southern coast of Nordaustlandet Island. At the same time, Hinlopen Strait was cleared of the ice completely. In the north, the ice edge shifted beyond 81° N.

In September 2019, the ice edge drift continued to move north (see Fig. 3, *b*). The ice drift, which was located in the southeast of the region under consideration, shifted into Hinlopen Strait, where it remained until the last third of September, when the direction of the prevailing winds changed.

---

[1] Frolov, I.E., ed., 2019. [*Quarterly Review of Hydrometeorological Processes in the Arctic Ocean – 3d Quarter 2019*]. Saint Petersburg: AARI, 71 p. (in Russian).

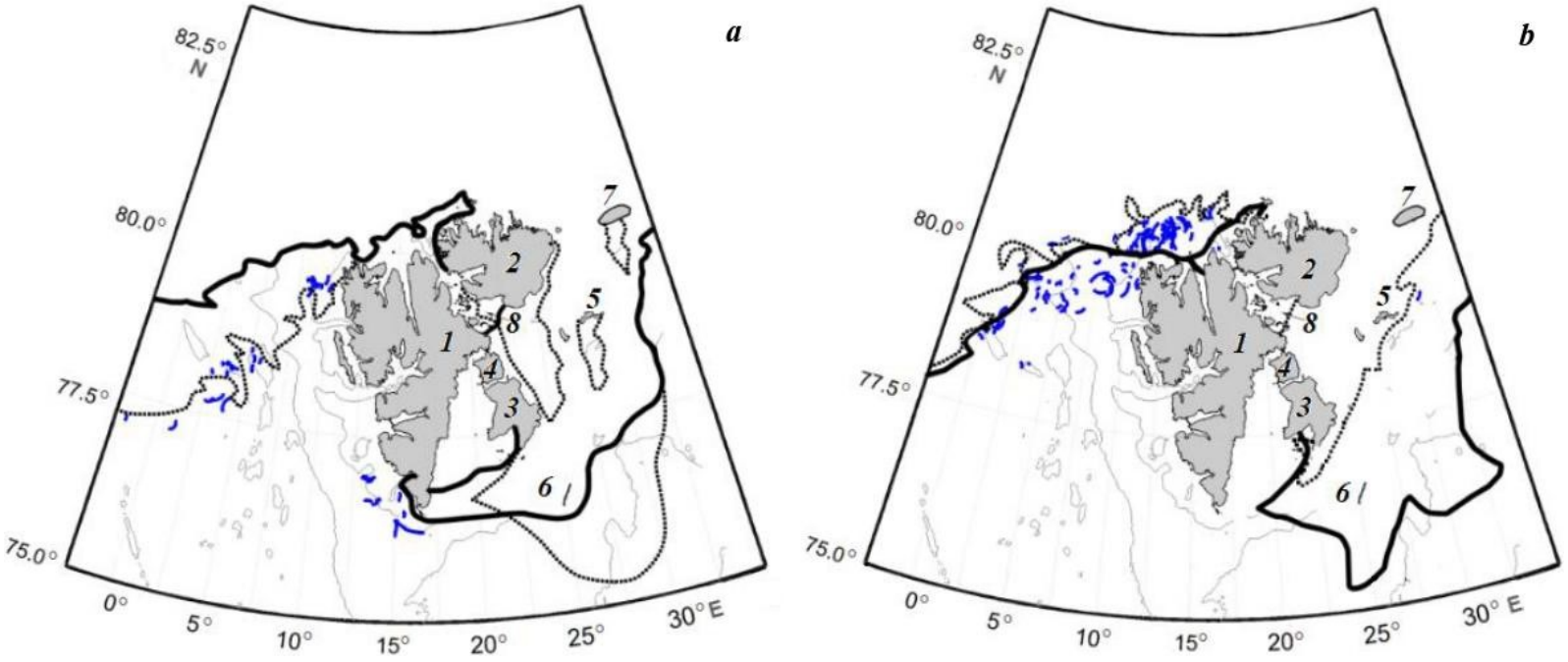

Fig. 2. Position of the ice edge boundary in June (*a*) and July (*b*) 2019: the solid line is for the beginning of the month; the dotted line is for the maximum southern position on 16 June 2019 (*a*) and at the end of July (*b*). The blue marks denote distribution of leading wave crests in the SIW packets. The numerals stand for: *1* – Spitsbergen Island; *2* – Nordaustlandet Island; *3* – Edge Island; *4* – Barents Island; *5* – King Charles Land; *6* – Hopen Island; *7* – White Island; *8* – Hinlopen Strait

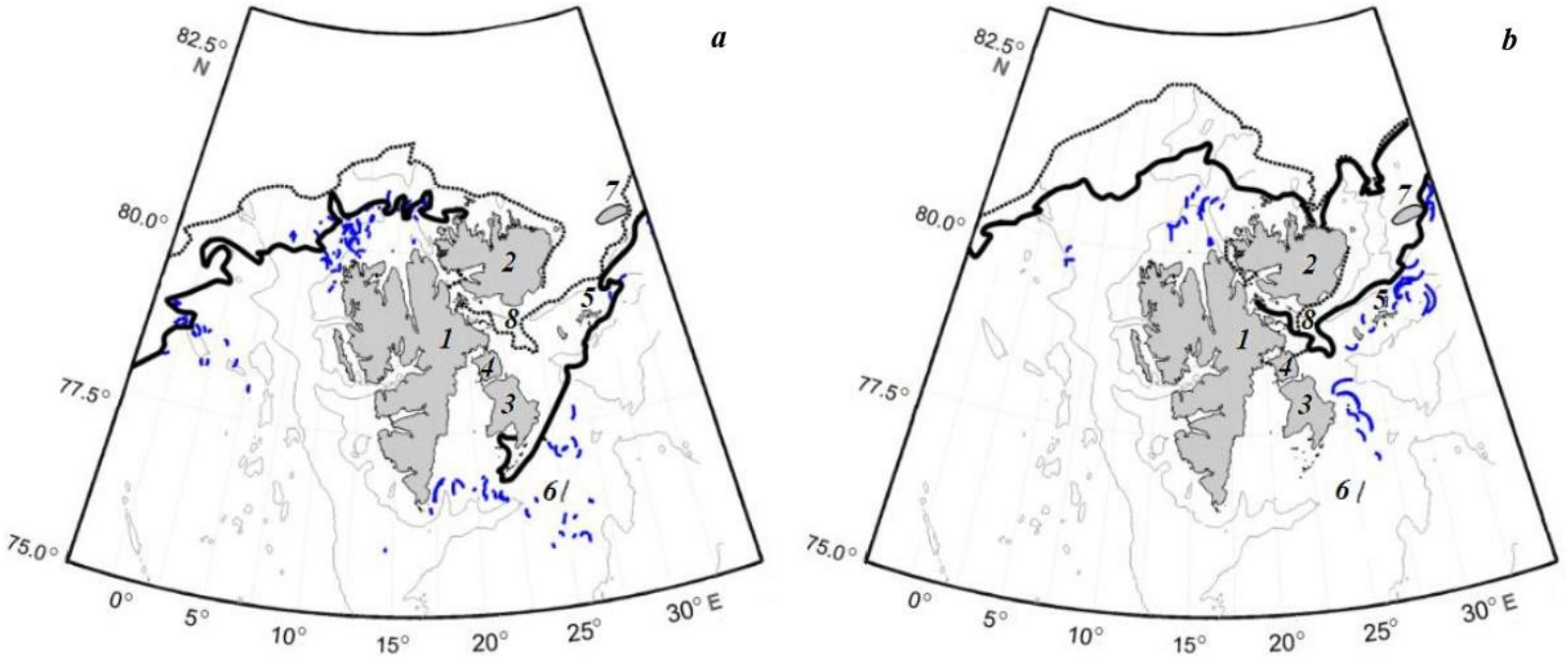

Fig. 3. Position of the ice edge boundary in August (*a*) and September (*b*) 2019: the solid line is for the beginning of the month; the dotted line is for the position at the end of August (*a*) and maximum northern position on 20.09.2019 (*b*). The blue marks denote distribution of leading wave crests in the SIW packets. The numerals stand for: *1* – Spitsbergen Island; *2* – Nordaustlandet Island; *3* – Edge Island; *4* – Barents Island; *5* – King Charles Land; *6* – Hopen Island; *7* – White Island; *8* – Hinlopen Strait

The maximum northern position (82° N) during the study period was reached by the ice edge on 16 September 2019. Within the next days, the direction of the shift of the ice edge drift changed to the opposite. As of the end of September 2019, in the north, the edge of the ice field was at 81.5° N.

Analysis of SAR observations of internal waves

During the processing of 1200 SAR images, 387 surface manifestations of SIWs were identified in June – September 2019. As a rule, internal waves were observed on RI in the form of packets of 4–5 waves with a characteristic decrease in the distance between them towards the packet tail; single solitons were recorded rarely.

The spatial distribution of leading wave crests in SIW packets in the study area during the warm period of 2019 is shown in Fig. 2 and Fig. 3 by the month and in Fig. 4 in total for the study period. The largest number of waves was detected in August (162 packets) and July (120 packets) (see Table). This is, apparently, due to more pronounced stratification of the upper layer of the ocean, which contributes to a more efficient SIW generation in these months.

In 2019, in the study region, internal waves were observed quite often in the shelf area northwest of Svalbard and in the deep part of Fram Strait. The SM of SIWs were also recorded to the south of Svalbard and near the eastern small islands of the island group of Kong Karls Land and the Kvitøya Island. Most packets were found in these regions.

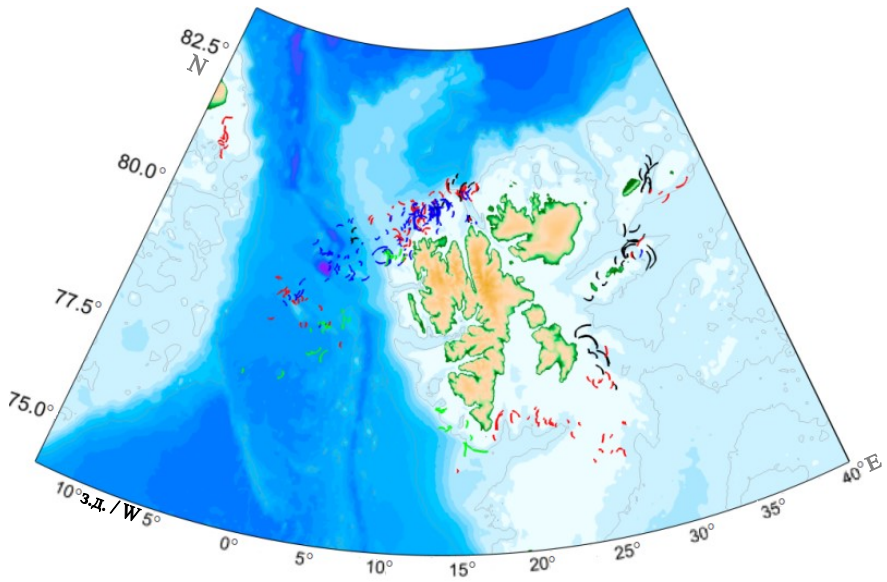

Fig. 4. Spatial distribution of leading wave crests in SIW packets in the study area in June – September 2019 (green– June; blue – July; red – August; black – September)

Number of surface manifestations of short-period internal waves in June – September 2019 identified on 1200 radar images

Month	Number of SM of SIW	Average number of waves per packet
June	44	5–6
July	120	4–5
August	162	5–6
September	61	6–7
Total	387	–

Fig. 5 shows the maps of the spatial distribution of total number of records of SIW packets (see Fig. 5, *a*) and probability of SIW manifestations (see Fig. 5, *b*) on a horizontal grid of 40 × 40 cells.

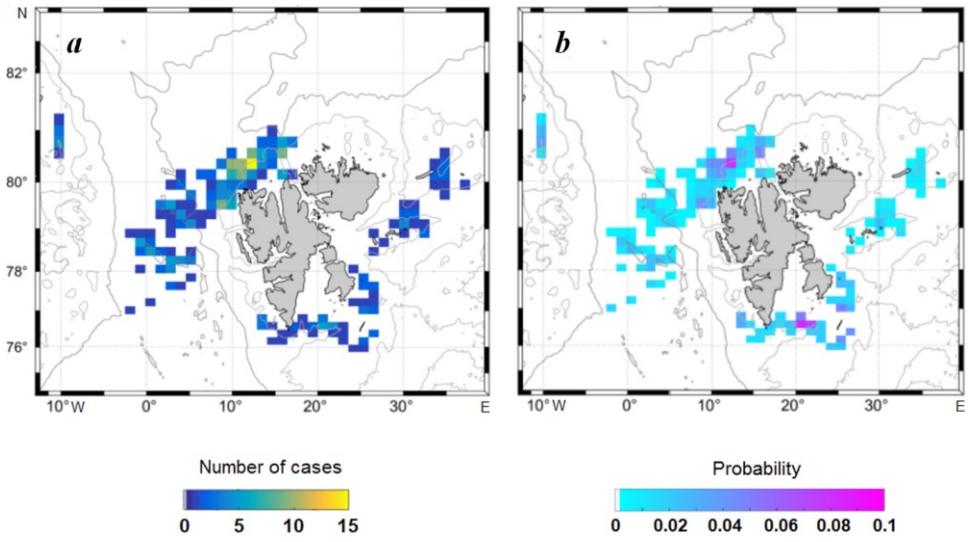

Fig. 5. Spatial distribution of internal wave characteristics in Fram Strait and near Svalbard: *a* – total number of records of SIW packets; *b* – probability of SIW manifestations on satellite radar images

The latter value was calculated as the ratio of the total number of registered SM of SIWs at a given grid node to the number of SAR images of this node. As can be seen from Fig. 5, *b*, the maximum values of SIW probability (~ 0.1) for the period under consideration are registered in the shelf area to the northwest and south of Svalbard.

Fig. 6 shows the maps of the spatial distribution of the mean values of the leading wave front length and the width of the SIW packets on a horizontal grid of 40 × 40 cells. As can be seen from Fig. 6, *a*, SIW packets with a leading wave front length of about 20–40 km were mainly observed in the water area in 2019.

The largest packets of internal waves were recorded at some distance from the areas with inhomogeneous topography, which, apparently, is associated with a more developed field of internal waves away from the immediate areas of IW generation. The maximum value of the leading wave front length (40 km) was registered south of Svalbard and the island group of Kong Karls Land. The SIW packets with the lowest values of this parameter within 1–5 km were recorded mainly near the edge of the ice field.

The width of the SIW packets varied from 1 to 12 km. The maximum values were registered south of Svalbard and the island group of Kong Karls Land. The minimum values from 1 to 5 km in most cases characterize the shelf area to the northwest of Svalbard.

The distribution histogram (Fig. 7, *a*) demonstrates clearly the high probability (more than 50% of all cases of observations) of the SIW front length in 2019 in the range from 10 to 12 km with a pronounced peak for the value of 10 km. The second peak of observations can be attributed to the values of the SIW front

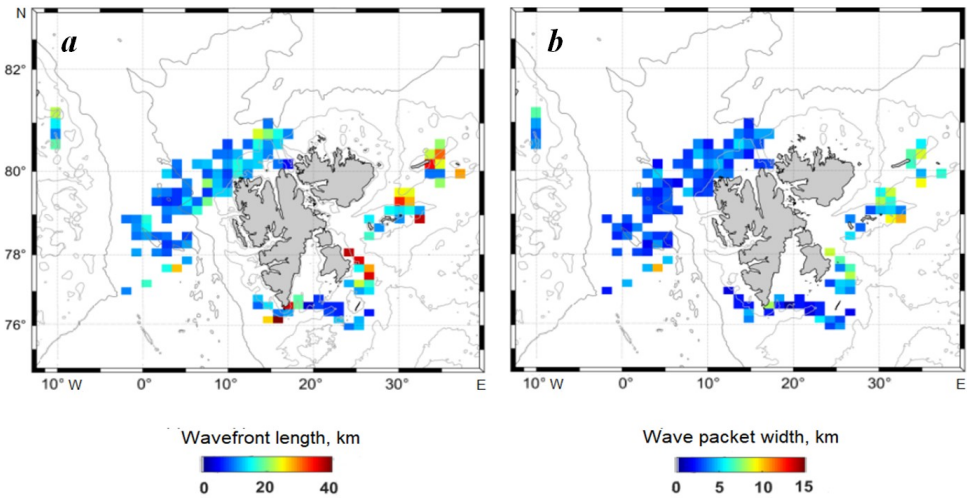

F i g . 6 . Spatial distribution of main parameters of internal waves in Fram Strait and near Svalbard in 2019: *a* – length of the leading wave front; *b* – packet width (km)

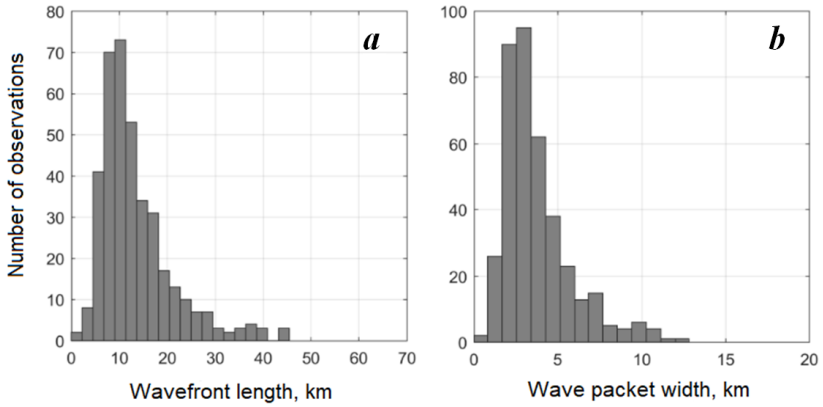

Fig. 7. Histograms of distributions of SIW main parameters in the study area in 2019: *a* – length of the leading wave front; *b* – SIW packet width (km)

length of about 7–8 km. Front length values from 20 to 30 km are found only in 15 % of cases. SIW front lengths from 40 to 50 km were recorded in very rare cases of 5 % only.

Histogram of distribution of SIW packet width (Fig. 7, *b*) shows that its greatest peak took place in the range of 3–4 km. Packet widths of 10–12 km were recorded extremely rarely, in 5 % of observations.

Results and discussion

Fram Strait and the waters adjacent to Svalbard are characterized by complex water dynamics and specific hydrological conditions, and the topography of the bottom of the study region has significant spatial inhomogeneity. The formation of density stratification is influenced greatly by the presence of a constant ice drift field, which undergoes shifts depending on the season and circulation variability in the polar region. In combination with tidal phenomena, all the above stated features of the study region create conditions for IW generation.

Based on SAR images, an analysis was made concerning the variability of the ice edge position in June – September 2019. It was found that in June 2019, ice spread in Fram Strait to the anomalous southern position off the western coast of Svalbard – up to 79° N. At the same time, the consolidated ice occupied the entire northern shelf area near Svalbard, which in July and August was freed from ice only up to 22° E, shifting to 81° N.

The maximum distance of the ice field from the archipelago was recorded in mid-September 2019 (82° N). The predominance of winds opposite to the ice drift direction in June – August 2019 explains rather high concentration of ice in the study region during this period.

387 SM of SIWs were recorded during the processing of 1200 SAR images. The largest number of SM of SIWs was recorded in August – 162 packets, which is apparently associated with more pronounced stratification of the upper layer of the ocean, which contributes to more efficient IW generation. Internal waves were observed on radar images in the form of packets of 4–5 solitons. The maximum lengths of the leading wave front were 30–40 km and were observed to the south of Svalbard. During the study period of 2019, short-period internal waves with leading wave front lengths of 7–10 km prevailed. The highest probability was noted for waves with a packet width of 3–4 km.

Comparison of the spatial distribution of the surface manifestations of SIWs and the ice edge drift position shows a good correlation (see Fig. 2, Fig. 3), which is confirmed by recent studies [15, 16]. Thus, in June 2019, SIWs were recorded in Fram Strait in deep water and at the southern extremity of the Spitsbergen Island in the immediate vicinity of the ice field edge. In July, SM of SIW were localized in a polynya opened to the north of the Spitsbergen Island, and in Fram Strait to the northwest of the archipelago, but much further to the north than in June.

In August, the position of the ice edge in the north slightly differed from that in July, and, accordingly, SM of SIWs were recorded almost within the boundaries of the same region with a slight shift in the SIW occurrence frequency to the east. To the south and east of Svalbard, SM of SIWs were also recorded mainly along the edge of the ice field, and to the south of the Spitsbergen Island – on the hydrographic polar front.

In September 2019, the main number of SIW manifestations was recorded to the east of Svalbard. At the same time, the length of their front was the largest for the period of the study observations. The generation of large SIW packets in this region was promoted by a combination of two following factors: the interaction of tidal currents and the East Spitsbergen Current with the features of the bottom topography near numerous small islands [2)] and the ongoing process of the melt of the ice preserved in Hinlopen Strait [17]. In September, to the north of the archipelago, at some distance from the ice edge, the minimum number of SM of SIW with short front lengths was recorded.

Conclusions

Horizontal and vertical density gradients, which can affect the generation and propagation of short-period internal waves, result from ice melt at the ice edge. Since the study region has a certain tidal regime, the interaction of the tidal current and the bottom topography with stratified water layer can also result in the emergence and distribution of internal waves. The combination of the above stated factors leads to the generation of the large SIW packets.

[2)] Troitskaya, Yu.I., 1995. [*Internal Wave Generation during Passing Round Irregularities by Stratified Shear Flows with Critical Layers*]. Report on Research Project. Grant no. 95-05-15325 (in Russian).

The tasks of future studies are to determine the temporal variability of the SIW parameters, to establish their connection with the tide phase, and to compare the obtained data with the results of numerical modeling using the *Arc5km*2018 model.

REFERENCES

1. Fer, I., Skogseth, R. and Geyer, F. Internal Waves and Mixing in the Marginal Ice Zone near the Yermak Plateau. *Journal of Physical Oceanography*, 40(7), pp. 1613–1630. doi:10.1175/2010JPO4371.1
2. Jardon, F.P., Bouruet-Aubertot, P., Cuypers, Y., Vivier, F. and Lourenço, A., 2011. Internal Waves and Vertical Mixing in the Storfjorden Polynya, Svalbard. *Journal of Geophysical Research: Oceans*, 116(C12), C12040. doi:10.1029/2010JC006918
3. Sundfjord, A., Fer, I., Kasajima, Y. and Svendsen, H., 2007. Observations of Turbulent Mixing and Hydrography in the Marginal Ice Zone of the Barents Sea. *Journal of Geophysical Research; Oceans*, 112(C5), C05008. doi:10.1029/2006JC003524
4. Svergun E.I. and Zimin, A.V., 2017. Forecast of the Occurrence of Intense Internal Waves in the White and Barents Seas according to Expeditionary Research. *Fundamentalnaya i Prikladnaya Gidrofizika = Fundamental and Applied Hydrophysics*, 10(2), pp. 13–19. https://doi.org/10.7868/S2073667317020022 (in Russian).
5. Bukatov, A.A., Solovei, N.M. and Pavlenko, E.A., 2021. Free Short-Period Internal Waves in the Arctic Seas of Russia. *Physical Oceanography*, 28(6), pp. 599–611. doi:10.22449/1573-160X-2021-6-599-611
6. Kozlov, I.E., Kudryavtsev, V.N., Zubkova, E.V., Atadjanova, O.A., Zimin, A.V., Romanenkov, D.A., Chapron, B. and Myasoedov, A.G., 2014. Generation Sites of Nonlinear Internal Waves in the Barents, Kara and White Seas from Spaceborne SAR Observasions. *Sovremennye Problemy Distantsionnogo Zondirovaniya Zemli iz Kosmosa*, 11(4), pp. 338–345 (in Russian).
7. Zubkova, E.V. and Kozlov, I.E., 2020. Characteristics of Short-Period Internal Waves in the Chukchi Sea Based on Spaceborne SAR Observations. *Sovremennye Problemy Distantsionnogo Zondirovaniya Zemli iz Kosmosa*, 17(4), pp. 221–230. https://doi.org/10.21046/2070-7401-2020-17-4-221-230 (in Russian).
8. Marchenko, A.V., Morozov, E.G., Kozlov, I.E. and Frey, D.I., 2021. High-Amplitude Internal Waves Southeast of Spitsbergen. *Continental Shelf Research*, 227, 104523. https://doi.org/10.1016/j.csr.2021.104523
9. Manley, T.O., Bourke, R.H. and Hunkins, K.L., 1992. Near-Surface Circulation over the Yermak Plateau in Northern Fram Strait. *Journal of Marine Systems*, 3(1–2), pp. 107–125. https://doi.org/10.1016/0924-7963(92)90033-5
10. Gascard, J.-C., Richez, C. and Rouault, C., 1995. New Insights on Large-Scale Oceanography in Fram Strait: The West Spitsbergen Current. In: W. Smith and J. Grebmeier, eds., 1995. *Arctic Oceanography: Marginal Ice Zones and Continental Shelves*. Washington: American Geophysical Union. Chapter 4, pp. 131–182. https://doi.org/10.1029/CE049p0131
11. Rudels, B., Korhonen, M., Schauer, U., Pisarev, S., Rabe, B. and Wisotzki, A., 2015. Circulation and Transformation of Atlantic Water in the Eurasian Basin and the Contribution of the Fram Strait Inflow Branch to the Arctic Ocean Heat Budget. *Progress in Oceanography*, 132, pp. 128–152. https://doi.org/10.1016/j.pocean.2014.04.003

12. Padman, L. and Dillon, T.M., 1991. Turbulent Mixing near the Yermak Plateau during the Coordinated Eastern Arctic Experiment. *Journal of Geophysical Research: Oceans*, 96(C3), pp. 4769–4782. doi:10.1029/90JC02260
13. Sandven, S. and Johannessen, O.M., 1987. High-Frequency Internal Wave Observations in the Marginal Ice Zone. *Journal of Geophysical Research: Oceans*, 92(C7), pp. 6911–6920. https://doi.org/10.1029/JC092iC07p06911
14. Kozlov, I.E. and Mikhaylichenko, T.V., 2021. Estimation of Internal Wave Phase Speed in the Arctic Ocean from Sequential Spaceborne SAR Observations. *Sovremennye Problemy Distantsionnogo Zondirovaniya Zemli iz Kosmosa*, 18(5), pp. 181–192. doi:10.21046/2070-7401-2021-18-5-181-192
15. Johannessen, O.M., Sandven, S., Chunchuzov, I.P. and Shuchman, R.A., 2019. Observations of Internal Waves Generated by an Anticyclonic Eddy: a Case Study in the Ice Edge Region of the Greenland Sea. *Tellus A: Dynamic Meteorology and Oceanography*, 71(1), 1652881. doi:10.1080/16000870.2019.1652881
16. Chunchuzov, I.P., Johannessen, O.M. and Marmorino, G.O., 2021. A Possible Generation Mechanism for Internal Waves near the Edge of a Submesoscale Eddy. *Tellus A: Dynamic Meteorology and Oceanography*, 73(1), pp. 1–11. doi:10.1080/16000870.2021.1947610
17. Ivanov, Yu.A., Mel'nikov, V.A. and Novitskiy, A.G., 1977. The Flow of Stratified Fluid over an Obstacle. *Izvestiya AN SSSR. Fizika Atmosfery i Okeana*, 13(12), pp. 1278–1286 (in Russian).

Submitted 5.04.2022; accepted after review 21.04.2022;
revised 27.04.2022; published 25.06.2022

About the authors:

Tamara V. Mikhaylichenko, Junior Research Associate, Marine Hydrophysical Institute of RAS (2 Kapitanskaya St., Sevastopol, 299011, Russian Federation), **ORCID ID**: **0000-0002-8696-9722**, **Scopus Author ID: 57358425100**, **AuthorID: 998530**, *fsbsi.mhi.tamara@yandex.ru*

Larisa A. Petrenko, Junior Research Associate, Marine Hydrophysical Institute of RAS (2 Kapitanskaya St., Sevastopol, 299011, Russian Federation), **ORCID ID**: **0000-0001-7246-9885**, **ResearcherID: AAY-6398-2020**, **Scopus Author ID: 7004614243**, *larcpetr@gmail.com*

Igor Y. Kozlov, Leading Research Associate, Marine Hydrophysical Institute of RAS (2 Kapitanskaya St., Sevastopol, 299011, Russian Federation), Ph.D. (Phys.-Math.), **ORCID ID**: **0000-0001-6378-8956**, **ResearcherID: G-1103-2014**, **Scopus Author ID: 49963767500**, *ik@mhi-ras.ru*

Contribution of the authors:

Tamara V. Mikhaylichenko – article concept development, analysis and interpretation of satellite data on SIW, article composition and writing, work on the final manuscript

Larisa A. Petrenko – article concept development, analysis and interpretation of satellite data on ice conditions, writing of the article section, work on the final manuscript

Igor Y. Kozlov – research task setting, analysis of results, participation in the article writing and arrangement, work on the final manuscript

All the authors have read and approved the final manuscript.